AD-A041 130 NORTHROP RESEARCH AND TECHNOLOGY CENTER HAWTHORNE CALIF F/G 11/3
OPTICAL COATINGS 2-6 MICRONS.(U)
MAY 77 P KRAATZ N00123-76-C-1321
UNCLASSIFIED NL

1 OF 1
AD A041130

END

DATE FILMED
7-77

26

OPTICAL COATINGS 2-6 MICRONS

Semi-Annual

Technical Report

May, 1977

44 p.

Progress rept. Jan-Mar 77

P. Kraatz
Principal Investigator

Prepared For

Naval Weapons Center

Contract No. N00123-76-C-1321

By

Northrop Research and Technology Center
3401 W. Broadway
Hawthorne, California 90250

1. INTRODUCTION

Progress during the third quarter (January, February, and March, 1977) under Contract No. N00123-76-C-1321 is reported here. The report is divided into three sections covering coating materials and deposition, coating properties (growth rates, refractive indices, and absorption coefficients) and future plans.

2. COATING MATERIALS AND DEPOSITION

Successful deposition of thin film coatings requires careful control of the evaporation technique and the associated parameters. Currently, thermal evaporation in a high vacuum is the technique that is most frequently used to deposit film coatings. Thermal evaporation in a high vacuum has been extensively developed, and two of the most common modes of evaporation are resistance heating and electron-beam heating. Both modes of evaporation are widely used, and it is relatively easy to produce good optical coatings. In spite of this favorable aspect, results of investigations of the properties of evaporated films have not always shown the expected consistency. The cause of these discrepancies probably does not lie in the method of evaporation itself, but rather in the lack of control of the many experimental parameters.

Evaporation from directly heated crucibles is widely and successfully used. By far the simplest and most common method is to make use of a boat of refractory metal which performs the dual function of a crucible and, when an electric current is passed through it, a heater. The selection of crucible materials, shapes, and designs is quite extensive. A great variety of crucibles suited to individual materials is produced and sold by specialized companies. Baffles sources, for example, are

used to evaporate and minimize the danger of spitting of SiO. Materials like ZnS can be evaporated from a howitzer source which is particularly useful in the infrared as its capacity can be very great.[1]

However, it has been found that some materials and to some extent the rather stable fluoride materials may react with the crucible used for their evaporation and this reaction may result in films having appreciable absorption.[2] The chance of a crucible reaction causing the deposited films to be absorbing is even greater for the oxide materials. For these materials there is also a good probability that dissociation causing absorption occurs due to overheating, especially if the evaporations are performed at very high temperatures to obtain high deposition rates.

If the material does not decompose at the evaporation temperature, then there are two main factors which govern the choice of crucible and heating method. The first is the temperature itself, and second is the tendency of the material to react with the crucible material. Materials which sublime at not too high a temperature can be heated in a crucible of alumina or even fused silica by radiation from above. A tungsten spiral, just above the surface of the material, can produce enough heat to vaporize it. Tantalum, molybdenum, and tungsten are all suitable for the manufacture of crucibles. Tantalum is the most frequently used and a wide range of materials can be evaporated from it. However, some materials react with it, (cerium oxide for example) and with molybdenum, and require the less reactive, but rather more difficult tungsten. PbF_2 will be reduced by hot tantalum, tungsten, or molybdenum crucibles, and it has to be evaporated from platinum or ceramic crucibles.

A method of evaporation which avoids many of the difficulties associated with directly and indirectly heated crucibles is electron-beam heating. In this method, the evaporant is contained in a suitable crucible or hearth of electrically conducting material, and is bombarded with a beam

of electrons to heat and vaporize it. The portion of the evaporant which is heated is in the center of the exposed surface, and there is a reasonably long thermal conduction path through the evaporant to the hearth, which can be held at a rather lower temperature than the melting point of the evaporant without prohibitive heat loss. This means that reaction between the evaporant and hearth can be inhibited; the hearth is frequently water-cooled to ensure this. Materials as reactive as silicon can be evaporated in this manner. The electrons are emitted by a hot tungsten filament and are attracted to the evaporant by a potential of several kilovolts. If the power is limited to the order of a kilowatt or so, it will be necessary to use an electrostatic or electromagnetic field to focus the electron-beam to a very small spot size in order to achieve reasonable evaporating rates. In this case, the temperature of the evaporant is extremely high and some evaporants can decompose at these elevated temperatures, causing absorption to appear in the condensed films. Decomposition of easily dissociating compounds can be prevented by increasing the spot size and increasing the power to achieve a reasonable rate of evaporation. However, this requires much high power approaching 10 kW, and possible disadvantages in this are the charging of the substrates and ionization of the evaporant material.[2] Therefore, some experimentation is required to establish the desired deposition rates which will allow the deposition of low absorbing films. A considerable amount of material has been written on electron-beam technology. Airco-Temescal has written a very informative thirty page booklet on this subject.[3]

The preparation of the materials to be evaporated is of considerable importance for the deposition of high quality optical coatings. Crucial properties are purity, gas content, and grain size. It is highly recommended that one use vacuum sintered and outgassed materials or even pieces of solid crystals to avoid gas outbursts and spattering during

the evaporation process. Powders are normally not suitable, since they have too much adsorbed gas which is desorbed during the heating and leads to pressure rise and spattering of the materials.

The quality of the optical coating materials depends on the purity of the starting materials and the method of preparation. Since impurities can increase optical absorption as well as initiate a variety of macroscopic or structural defects, commercial materials of highest purity must be used. The purity is frequently given in percentage of the main material, up to 99.9999%; the remainder consisting of unknown impurities. Although this number indicates ultrapure material, it still contains a great number of impurity atoms per cubic centimeter. It is, therefore, necessary to know the kind and concentratration of all impurities. A variety of methods exist for the detection and determination of impurity concentration.[4] The most important are x-ray, optical absorption, and mass spectroscopy. Knowing the impurities present, it is essential to determine which ones actually influence the respective properties. These impurities must be removed or at least reduced in concentration.

Coating materials of desired purity are only available when a material has attained broad application. In most cases, it has to be purified; this is quite an involved operation. Drying is very essential if the material is contaminated by water in any form. The effects of absorbed moisture are so pronounced that they completely mask the normal aging and the basic loss mechanism. Absorbed or trapped water or hydroxyl ions can be eliminated by drying under vacuum and slowly increasing the temperature to the level at which the loosely bound water is removed by diffusion and evaporation. True oxide or hydroxide compounds in solid form are not removable by this means, but require chemical reaction in some form, (i.e., scavenging by a reactive atmosphere).

Coating materials employed to date in the program are listed and identified as to source and nominal purity in Table 1. In all cases, these materials represent the highest purity commercially available. No attempt was made to further purify any of these materials.

Clean substrate surfaces are a prerequisite for successful coatings. The slightest amount of contamination can cause an immense amount of harm in the coating deposition process as well as an increase in surface absorption. Cleaning is an art rather than a science and, therefore, there is a great diversity of opinion on what constitutes a "good" procedure for cleaning substrates prior to coating them. A full treatment of various methods for cleaning glass substrates is given by Holland.[5] However, the sensitive nature of the highly polished surfaces of the fluoride windows requires the avoidance of such harsh cleaning procedures, since serious damage to the delicate optical surfaces can be the result of improper cleaning techniques.

The cleaning process utilized at Northrop to clean the fluoride windows prior to the deposition of the coating has been more or less conventional. Before the windows are placed into the system for coating, they are cleaned in a solution of detergent and warm water, then rinsed with distilled water and alcohol and blown dry with nitrogen gas. The coating system is pumped down to a pressure of less than 10^{-6} Torr and a pressure of less than 5×10^{-6} Torr is maintained during the coating deposition. The windows are heated to the desired substrate temperature and just prior to coating deposition they are subjected to a glow discharge cleaning. So far this procedure has been adequate for cleaning the fluoride surfaces prior to the deposition of antireflection coating designs.

In the vacuum deposition of thin films by an evaporation process, knowledge of the substrate temperature and its control is often very important.

TABLE 1. COATING MATERIALS

Al_2O_3	Random Chunks of UV-Grade Sapphire, Union Carbide Corporation, San Diego, Calif.
LaF_3	Hot-Pressed Tablets, 99.9% Purity, Balzers High Vacuum Corp., Santa, Ana, Calif.
MgF_2	Fused Granules, 99.99% Purity, Balzers High Vacuum Corp., Santa Ana, Calif.
MgO	Hot-Pressed Tablets, 99.95% Purity, Balzers High Vacuum Corp., Santa Ana, Calif.
PbF_2	Fused Granules, 99.99% Purity, Balzers High Vacuum Corp., Santa Ana, Calif.
SiO	Linde Select Grade, R. D. Mathis Company, Long Beach, California.
SrF_2	Random Chunks, Optical Grade, EMCO Sales, Anaheim, California.
ThF_4	Fused Granules, 99.9% Purity, CERAC, Milwaukee, Wisconsin.
ThF_4	Fused Granules, 99.9% Purity, Balzers, High Vacuum Corp., Santa, Ana, Calif.
ZnS	Hot-Pressed Tablets, 99% Purity, Balzers High Vacuum Corp., Santa Ana, Calif.
ZnSe	Granules, 99.99% Purity, Balzers High Vacuum Corp., Santa Ana, Calif.

In fact, the substrate temperature plays an especially important role for the whole condensation process. It controls the surface mobility of the condensing atoms or molecules and determines the degree of disorder of the growing film. Film adhesion and durability are improved by heating the substrates prior to and during deposition. Of paramount importance is the removal of adsorbed gases from the substrate. Thus water removal is one of the main reasons for heating substrates prior to deposition.

In practice a wide range of substrate temperatures is employed. The deposition of metal oxides requires substrate temperatures of approximately 300°C to obtain optimal film properties.[2] On the other hand, zinc sulfide should be deposited at a substrate temperature below 180°C to provide a compromise between reevaporation and film durability.[6] If a low substrate temperature is required to obtain a desired film property such as minimal scattering, and if this temperature is too low to remove water vapor from the substrate, then the substrate can be preheated to remove the water vapor and subsequently cooled to the required deposition temperature. Glow discharge cleaning can also be used in this situation.

Since the index of refraction of the films and film structure are a function of substrate temperature, it is important that both substrates and monitoring pieces be maintained at a uniform and constant temperature throughout the deposit cycle. A typical substrate heater is described by Mattauch[7] and the measurement and control of substrate temperature is discussed by Hanson, et. al.[8]

The objective in vacuum evaporation is nearly always to deposit films to certain specifications. If the specification is primarily one of thickness, it is sufficient to determine when the accumulated deposit has reached the desired value so that the deposition process can be terminated. However,

intensive film properties such as density, stress, crystallinity, and index of refraction depend on the rates at which the evaporant and residual gas molecules arrive at the substrate. It is therefore necessary to maintain specified evaporation rates. The influence of the deposition rates on the index of refraction of SiO has been studied by Hass, et. al.[9] A high rate of deposition corresponds to a high index of refraction, whereas, a slow rate of deposition corresponds to a low index of refraction.

Reviews of thickness and rate monitors have been given by Steckelmacher[10] and Behrndt.[11] The control of evaporation rate is a more complex task than thickness control because it requires adjustment of the source temperature.

All coating depositions required for this program were carried out in a commercial vacuum system (Balzers Model 710) which is equipped with an oil diffusion pump and a liquid nitrogen trap. This system is capable of routinely maintaining pressures of the order of 10^{-6} Torr and is equipped with a substrate heater and a thin film monitor to control deposition rate and film thickness. Proper control of the thickness of each layer is afforded by observing the reflectance at the control wavelength of a suitably positioned monitor plate in the coating chamber and stopping deposition when the reflectance reaches a predetermined level. In all cases, care is taken to ensure the uniformity of the thickness of the layers. In order to obtain uniform layers, the window substrates are rotated above the evaporation source during the deposition process.

Deposition parameters utilized in this program are summarized for each material in Table 2. Electron beam heating was employed in the evaporation of slightly more than half of the materials, while thermal evaporation from a boat was utilized in the balance of the cases.

TABLE 2. DEPOSITION PARAMETERS

MATERIAL	METHOD OF EVAPORATION	SUBSTRATE TEMPERATURE	DEPOSITION PRESSURE (TORR)	DEPOSITION RATE
Al_2O_3	E-Beam	200°C	5×10^{-5}	~600 Å/Min
LaF_3	Mo Boat	200°C	8×10^{-6}	~1800 Å/Min
MgF_2	E-Beam	200°C	2×10^{-6}	~1800 Å/Min
MgO	E-Beam	200°C	6×10^{-5}	~1200 Å/Min
PbF_2	E-Beam	200°C	7×10^{-6}	~1800 Å/Min
SiO	Ta Boat	200°C	$<1 \times 10^{-6}$	~3000 Å/Min
SrF_2	Mo Boat	200°C	8×10^{-6}	~1800 Å/Min
ThF_4	E-Beam	200°C	4×10^{-6}	~1800 Å/Min
ZnS	Ta Boat	150°C	8×10^{-6}	~1800 Å/Min
ZnSe	Ta Boat	150°C	4×10^{-6}	~1800 Å/Min

3. COATING PROPERTIES

The coating properties of interest in this study include refractive index, absorption coefficient, crystal structure and preferred orientation, and relative growth rates on the various substrate materials and orientations. In order to determine these properties, single layer films of quarterwave and halfwave optical thickness at appropriate wavelengths (3.8 μm and/or 5.3 μm) were deposited on one surface of CaF_2 and/or SrF_2 substrates having nominal (100), (110), and (111) orientations.

Refractive indices were obtained from infrared transmission measurements of the quarterwave films, while absorption coefficients were measured on the halfwave films. Information on relative growth rates is obtained from spectrophotometer transmission scans of the halfwave coated samples in the visible region (600 to 800 nm), where the interference effects of the coatings are more pronounced. Data on film structure and preferred orientation are obtained using x-ray diffraction. Refractive index, growth rate, and absorption results are reported here. Structure and preferred orientation results will be included in the next quarterly report.

Spectrophotometer scans from 600 to 800 nm of halfwave optical thickness films at 3.8 or 5.3 μm on CaF_2 and SrF_2 substrates are presented in figures 1 through 18. The position (wavelength) of maxima and minima in the transmission of these materials is related to the higher order interference of the coating on a given substrate orientation. Shifts in transmission maxima (or minima) towards longer wavelengths are indicative of greater optical thickness on a particular substrate orientation; shifts toward shorter wavelengths indicate lesser optical thickness. Since the refractive index of all the coating materials (except MgO) is independent of substrate orientation and all films were deposited simultaneously on three different orientations of a given substrate material, differences

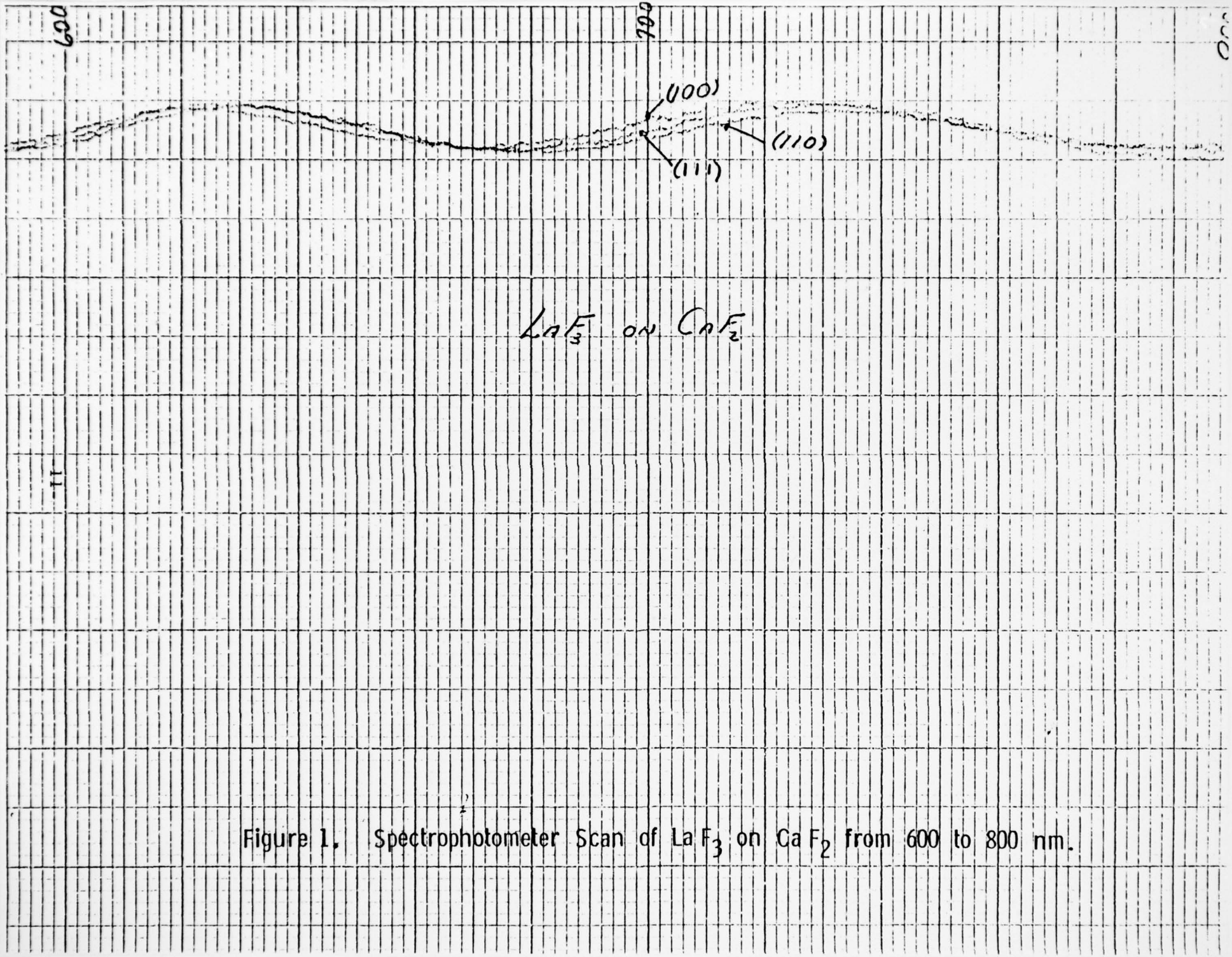

Figure 1. Spectrophotometer Scan of LaF_3 on CaF_2 from 600 to 800 nm.

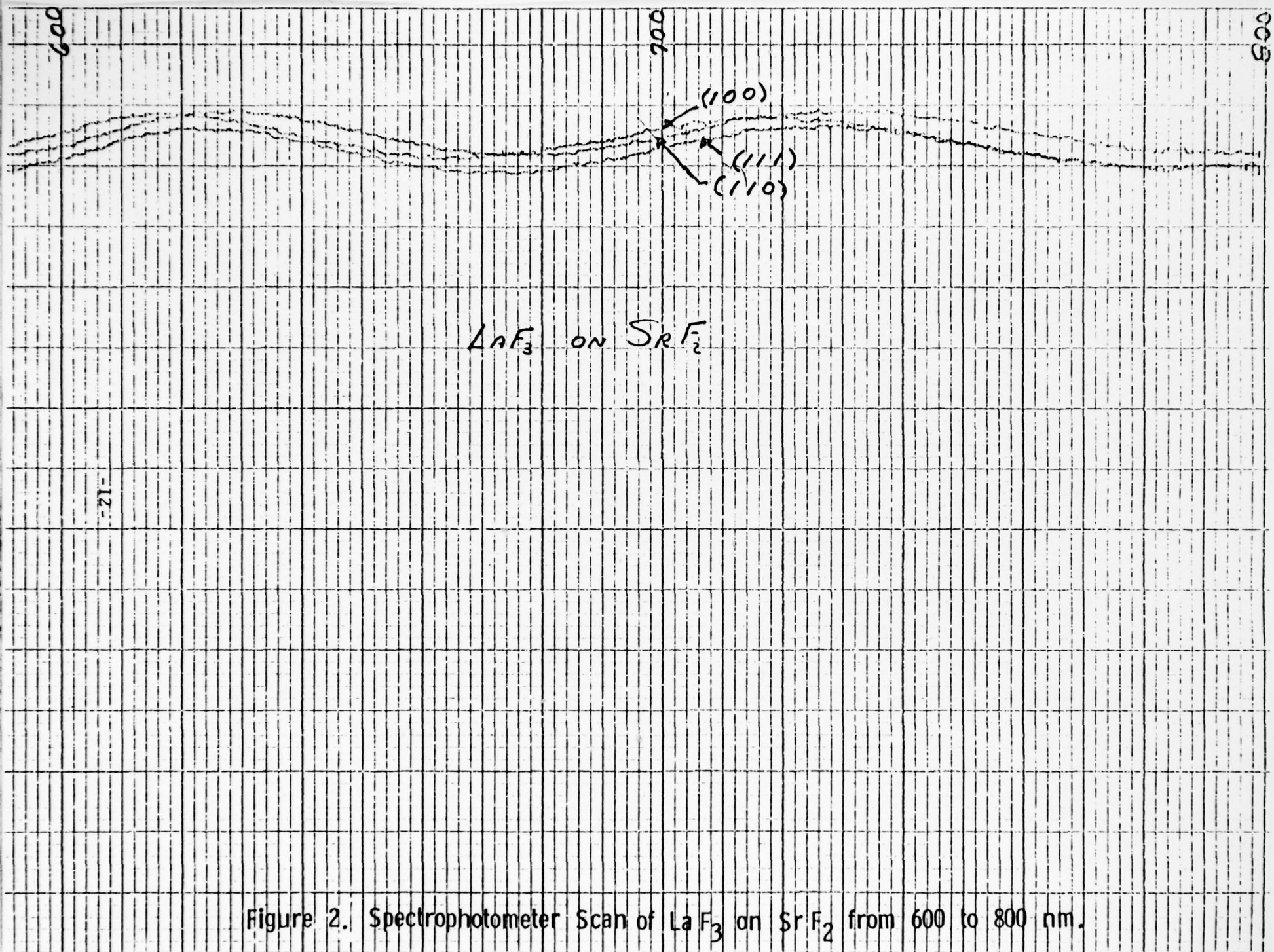

Figure 2. Spectrophotometer Scan of LaF_3 on SrF_2 from 600 to 800 nm.

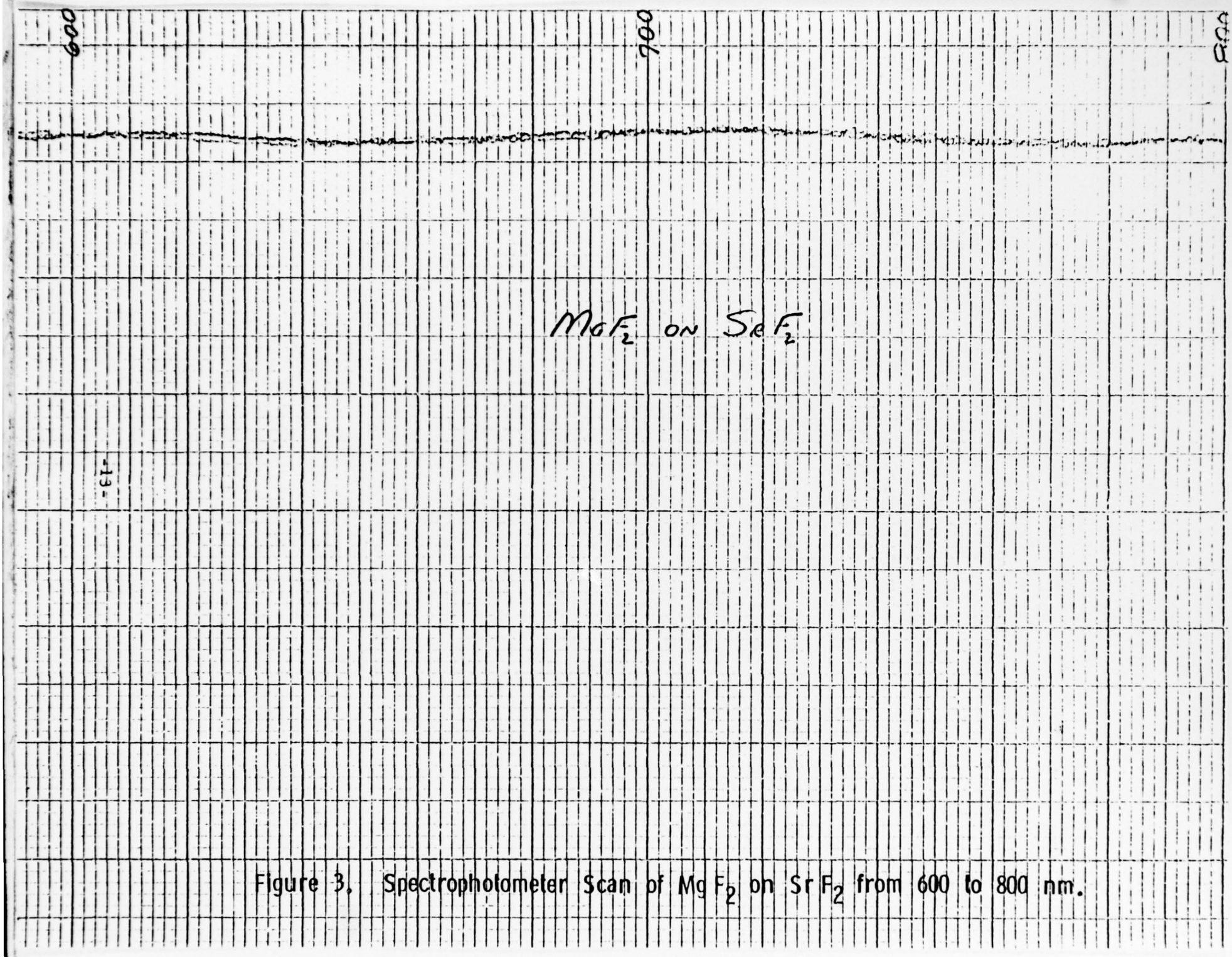

Figure 3. Spectrophotometer Scan of MgF_2 on SrF_2 from 600 to 800 nm.

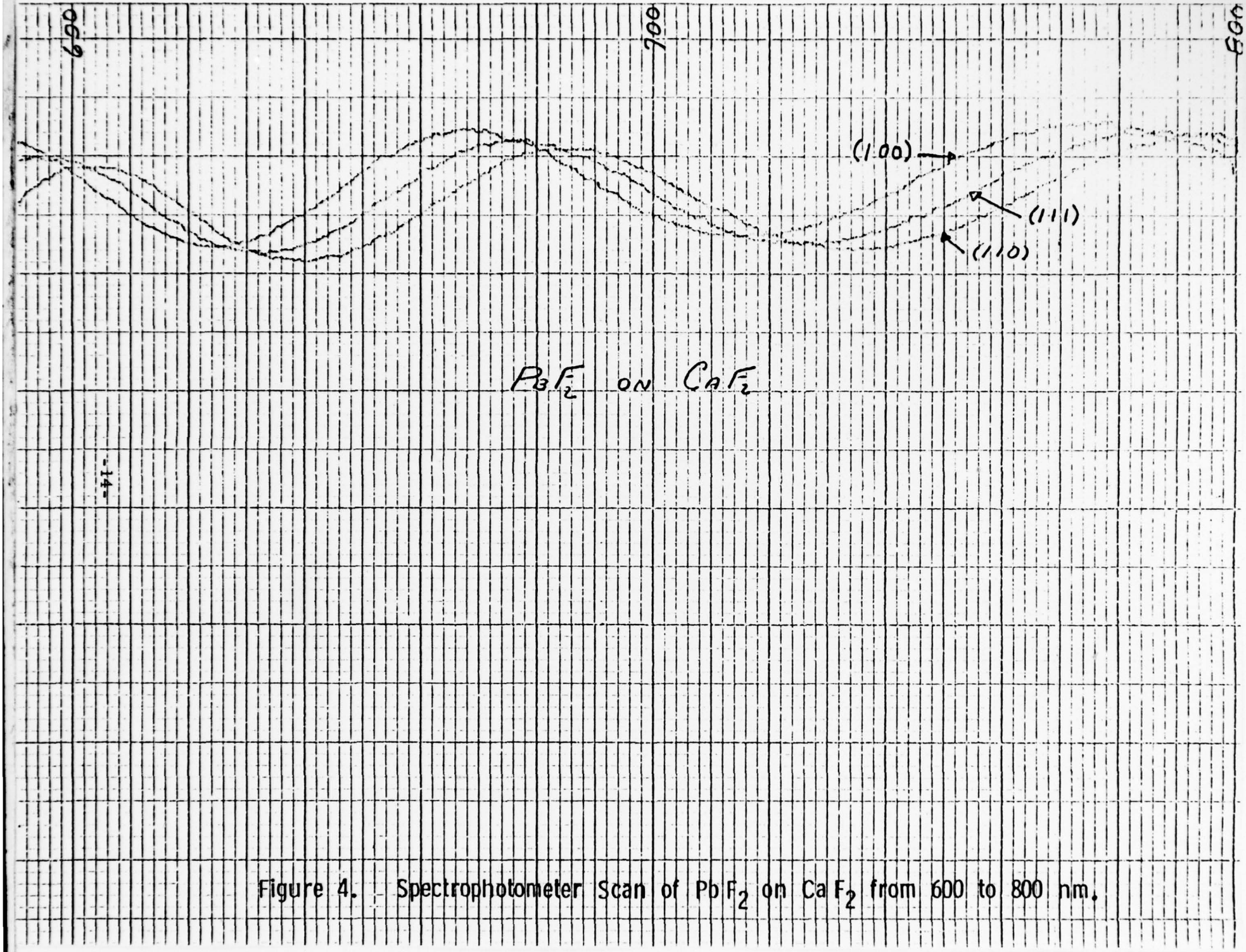

Figure 4. Spectrophotometer Scan of PbF_2 on CaF_2 from 600 to 800 nm.

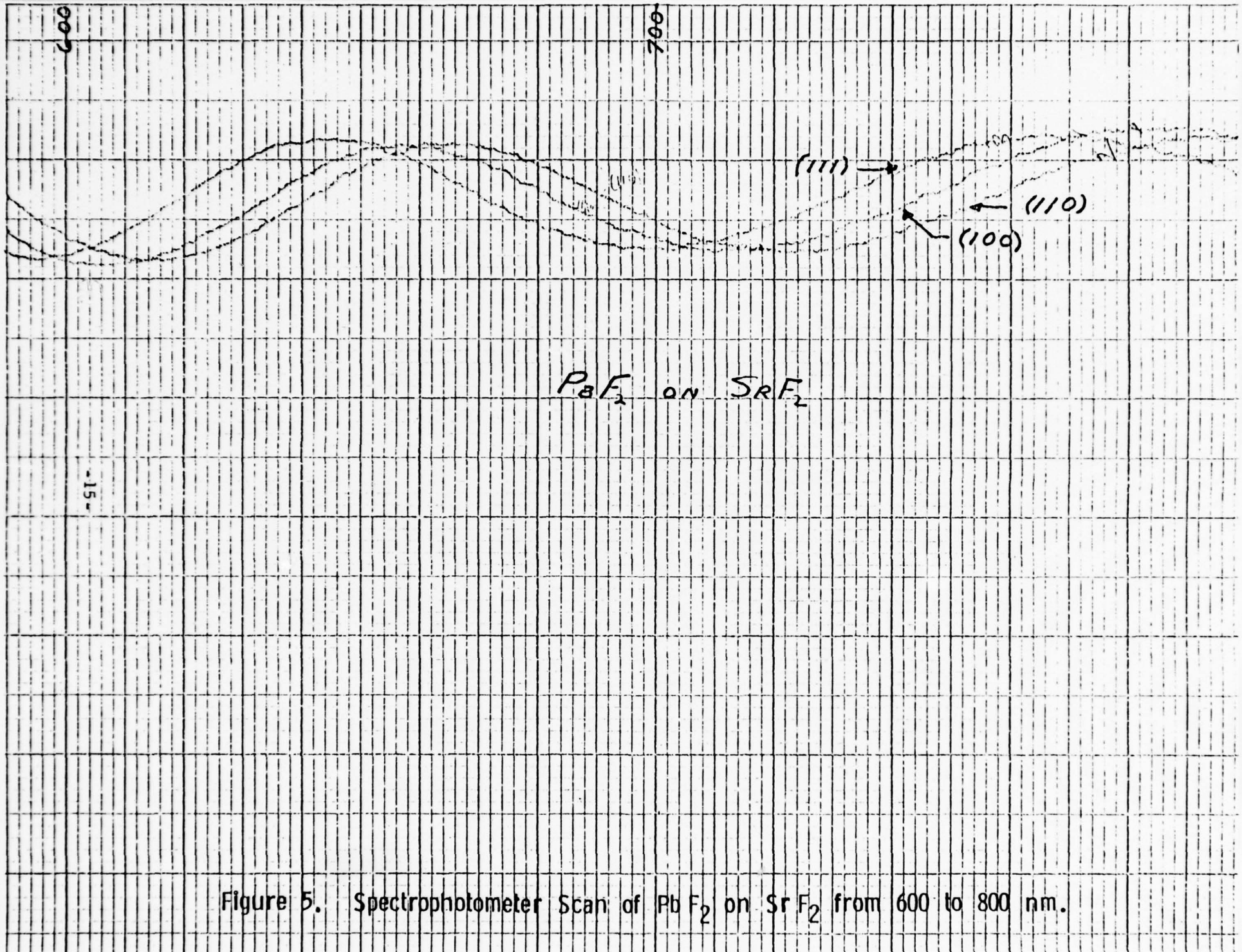

Figure 5. Spectrophotometer Scan of PbF_2 on SrF_2 from 600 to 800 nm.

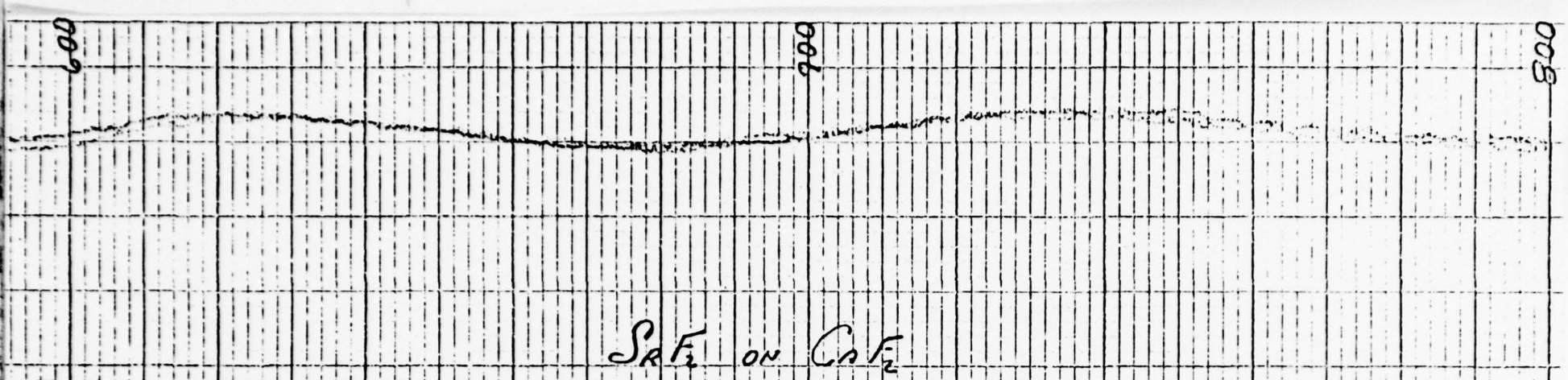

Figure 6. Spectrophotometer Scan of SrF_2 on CaF_2 from 600 to 800 nm.

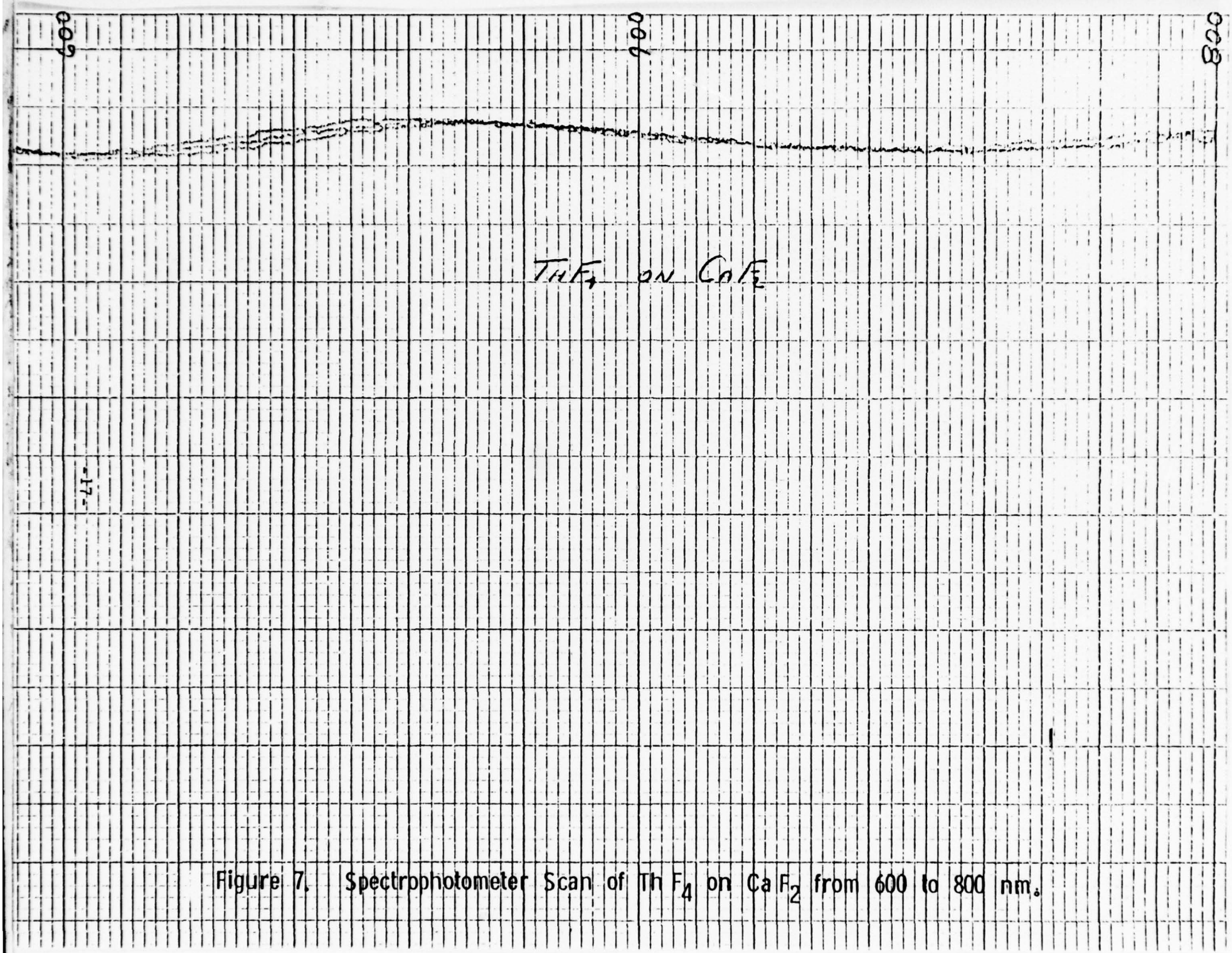

Figure 7. Spectrophotometer Scan of Th F_4 on Ca F_2 from 600 to 800 nm.

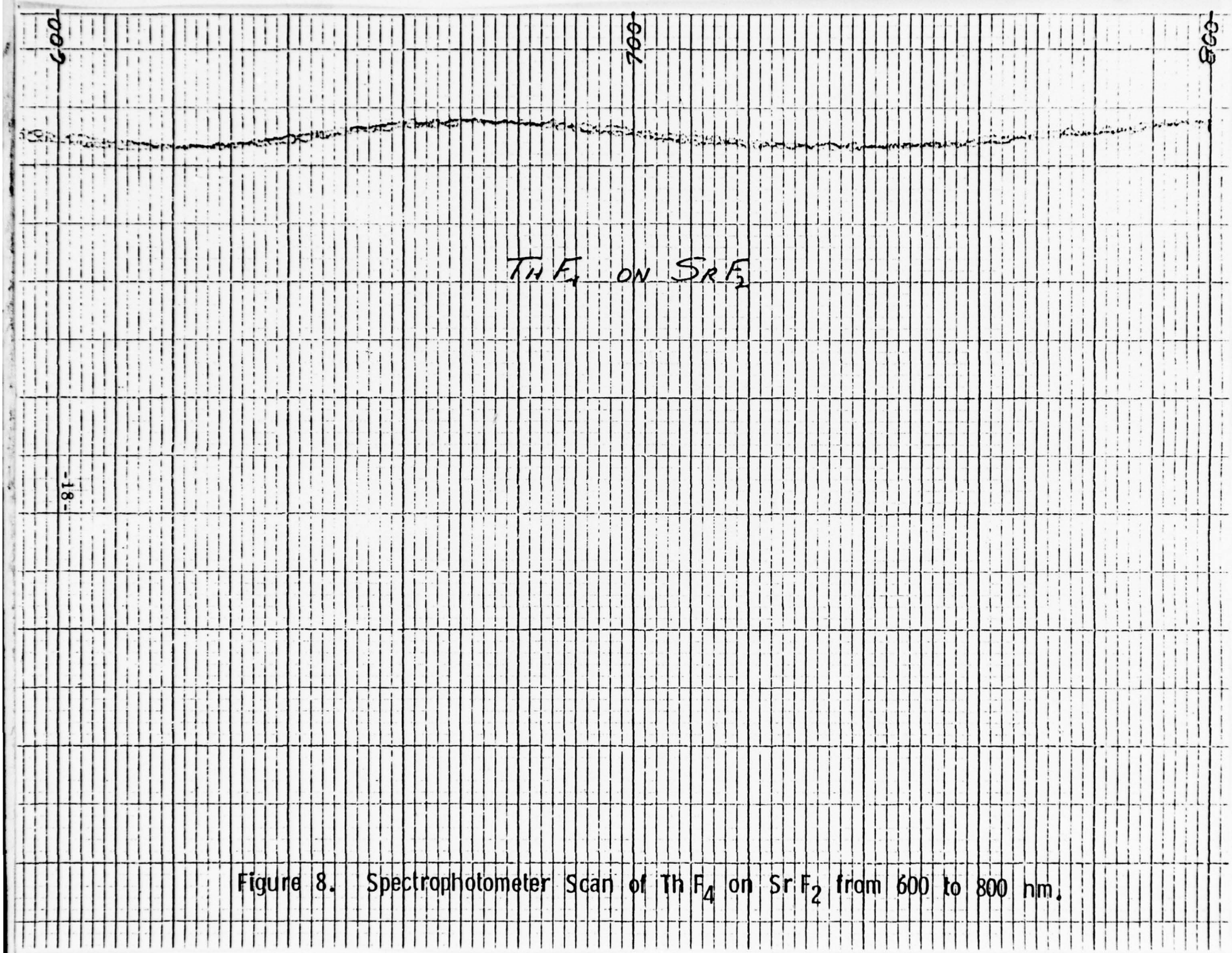

Figure 8. Spectrophotometer Scan of ThF_4 on SrF_2 from 600 to 800 nm.

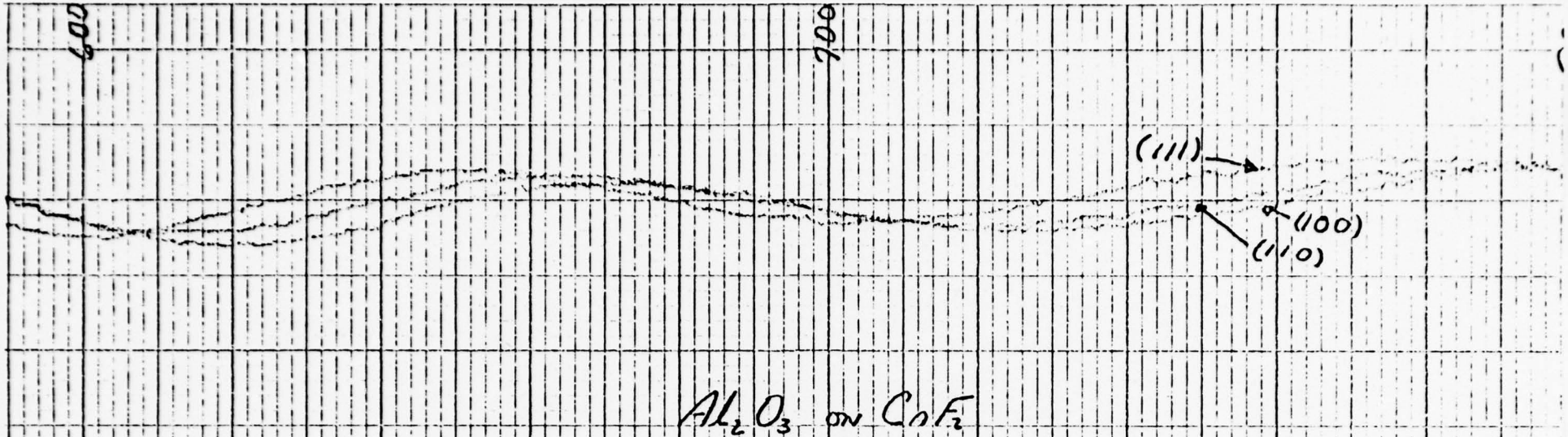

Figure 9. Spectrophotometer Scan of Al_2O_3 on CaF_2 from 600 to 800 nm.

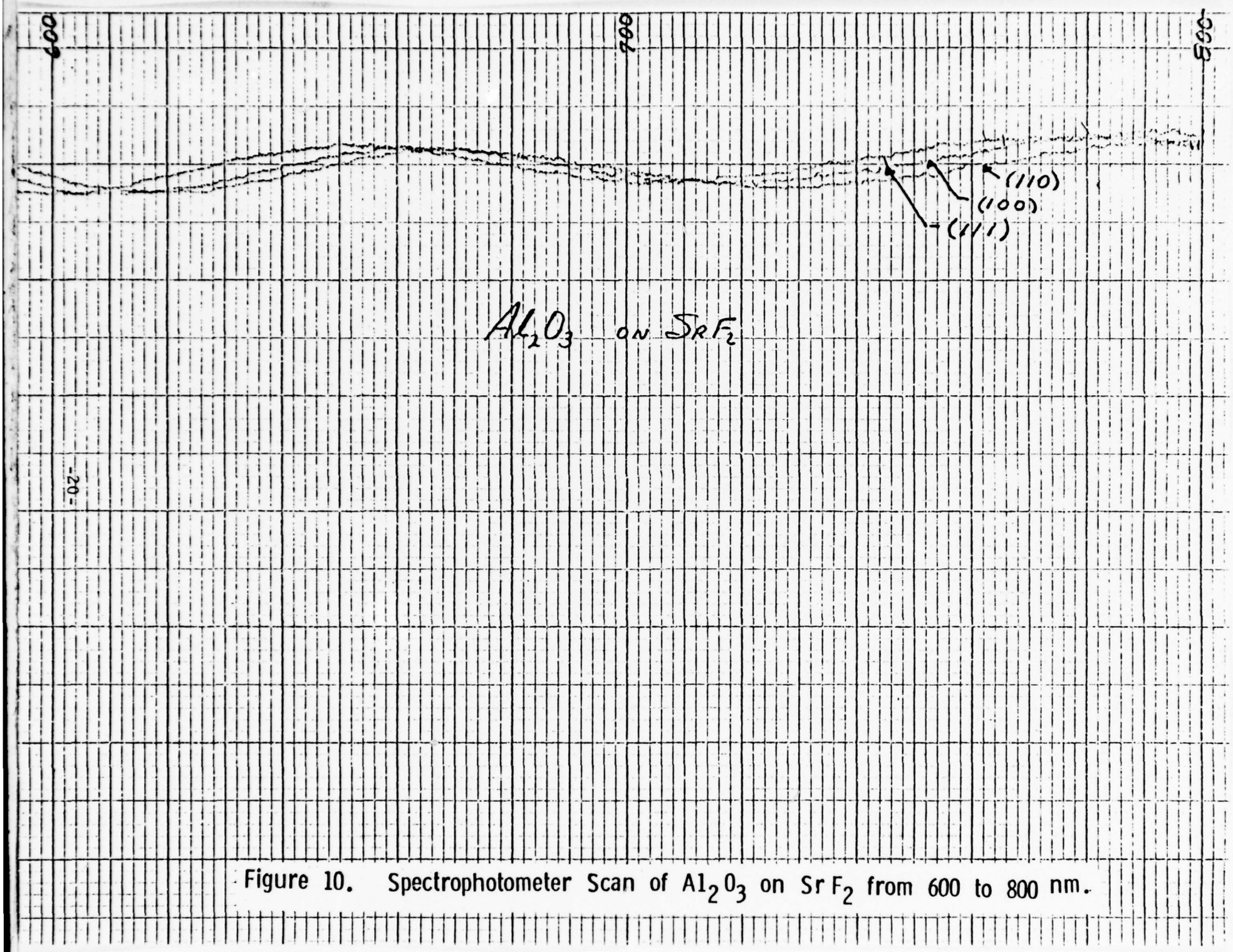

Figure 10. Spectrophotometer Scan of Al_2O_3 on SrF_2 from 600 to 800 nm.

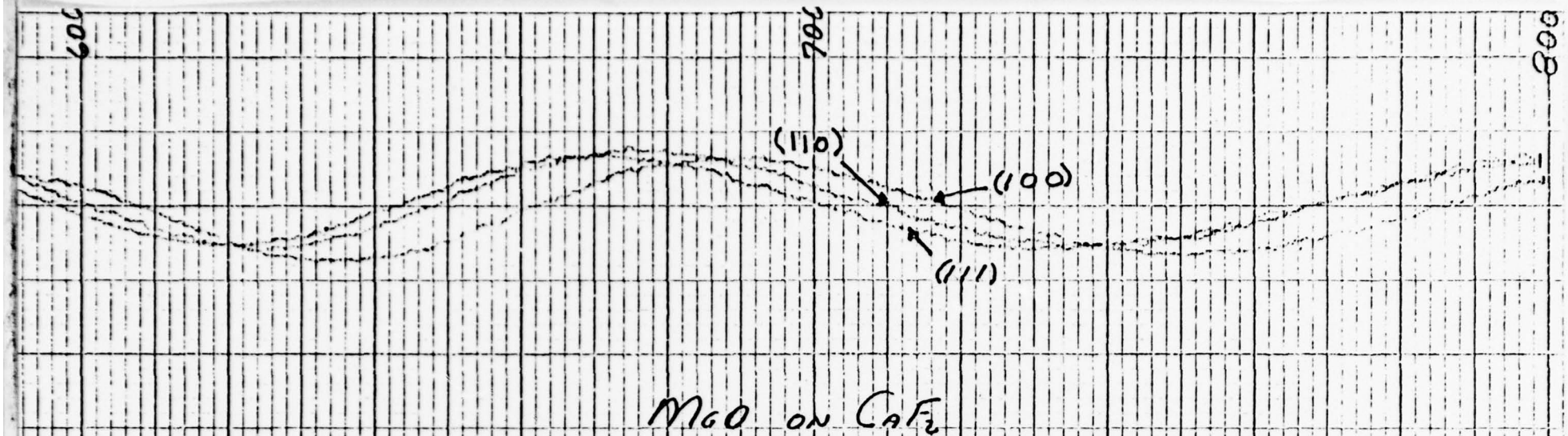

Figure 11. Spectrophotometer Scan of Mg O on CaF_2 from 600 to 800 nm.

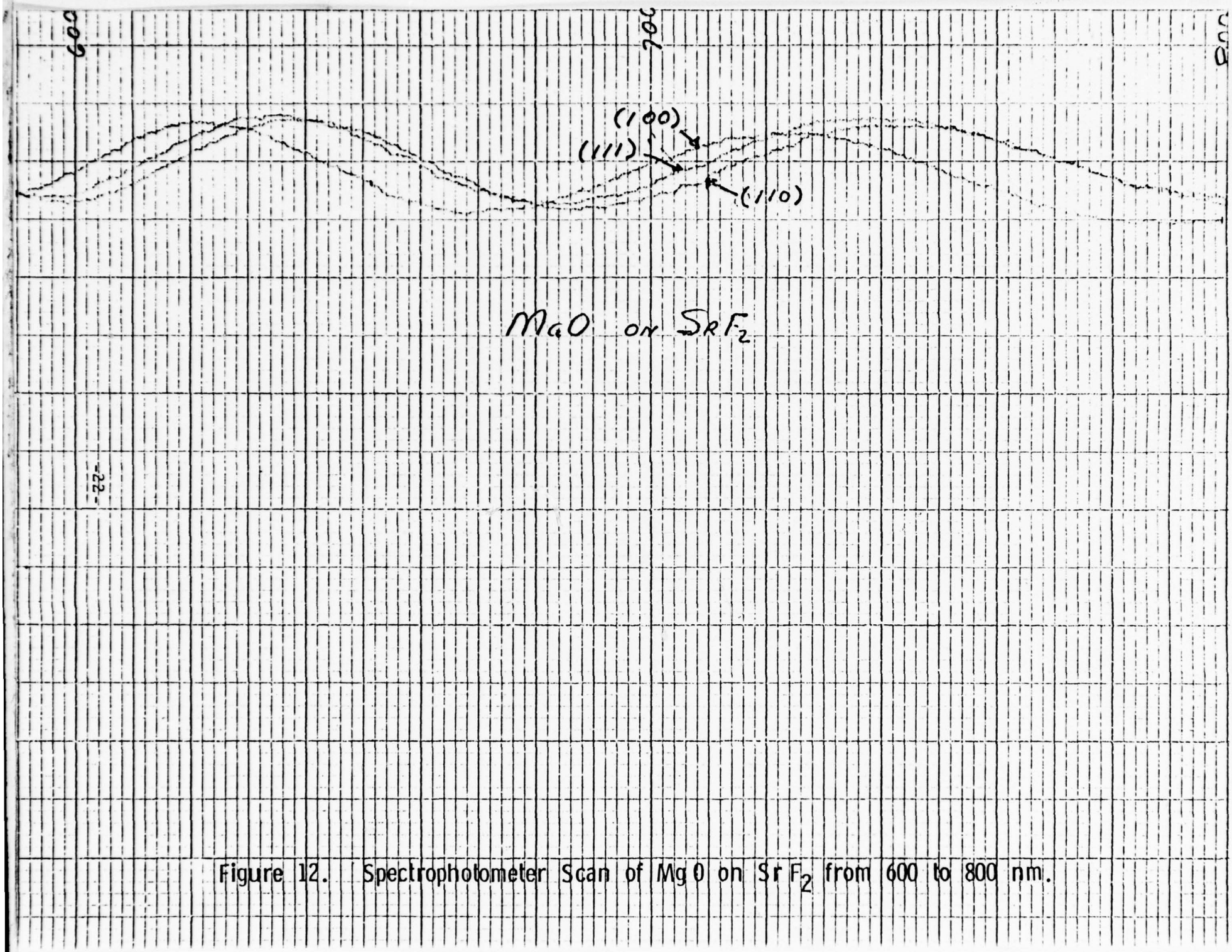

Figure 12. Spectrophotometer Scan of Mg O on SrF_2 from 600 to 800 nm.

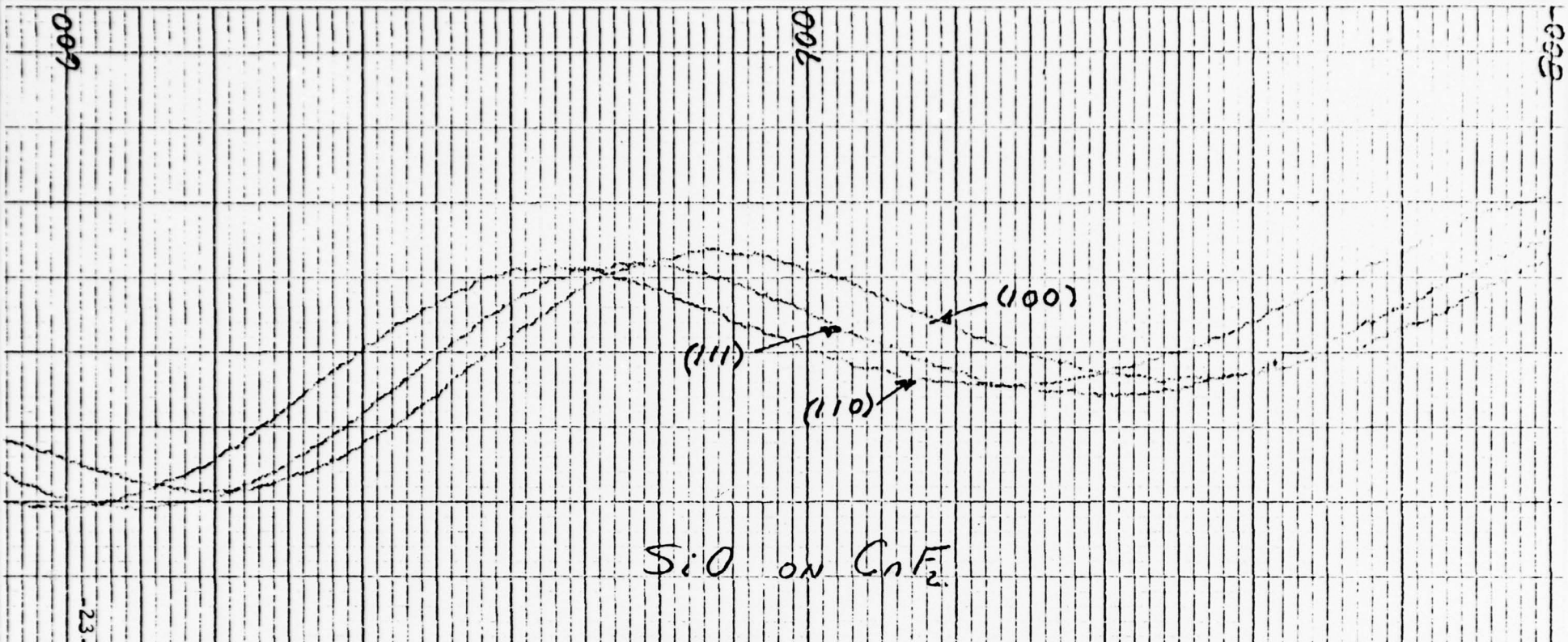

Figure 13. Spectrophotometer Scan of SiO on CaF_2 from 600 to 800 nm.

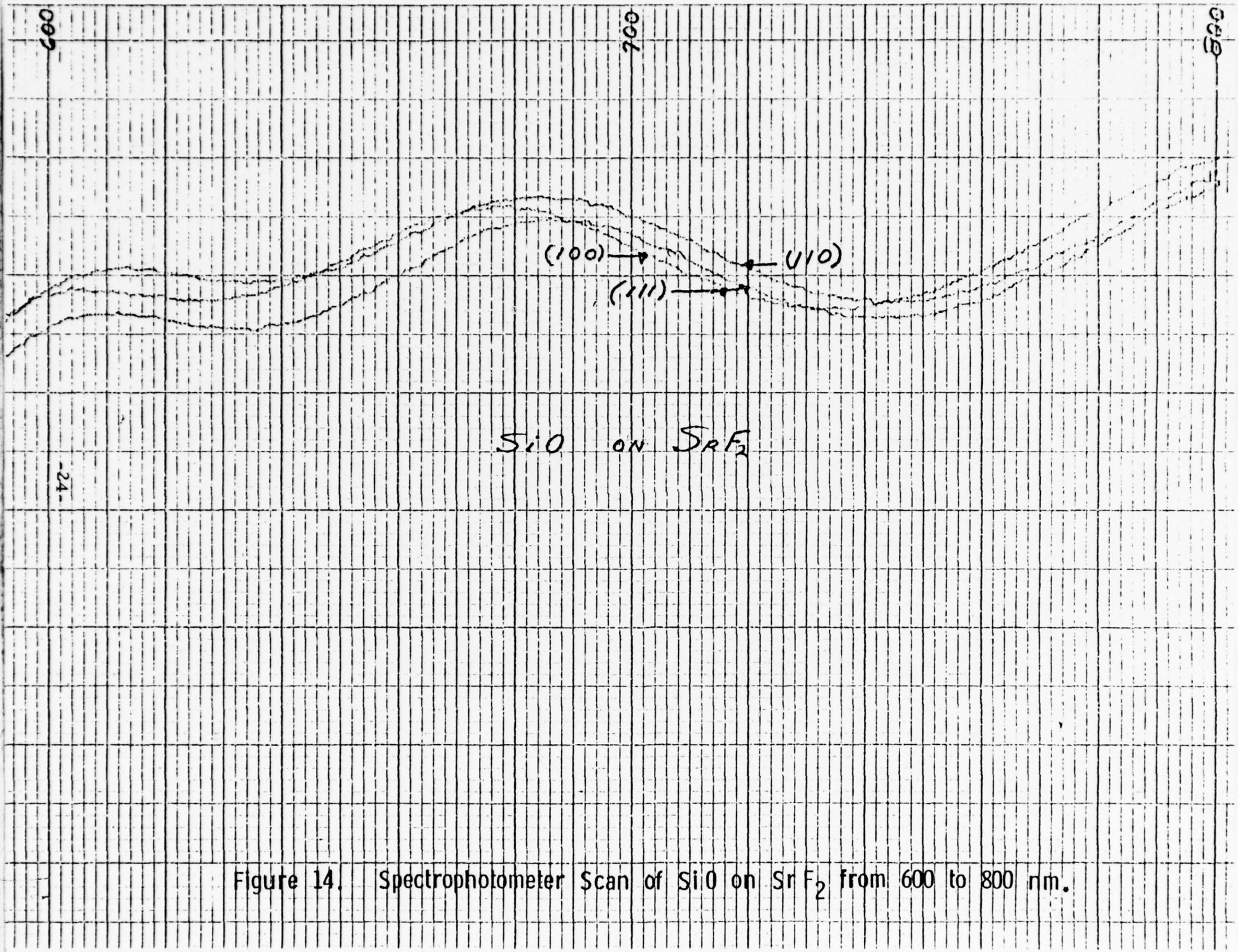

Figure 14. Spectrophotometer Scan of SiO on SrF_2 from 600 to 800 nm.

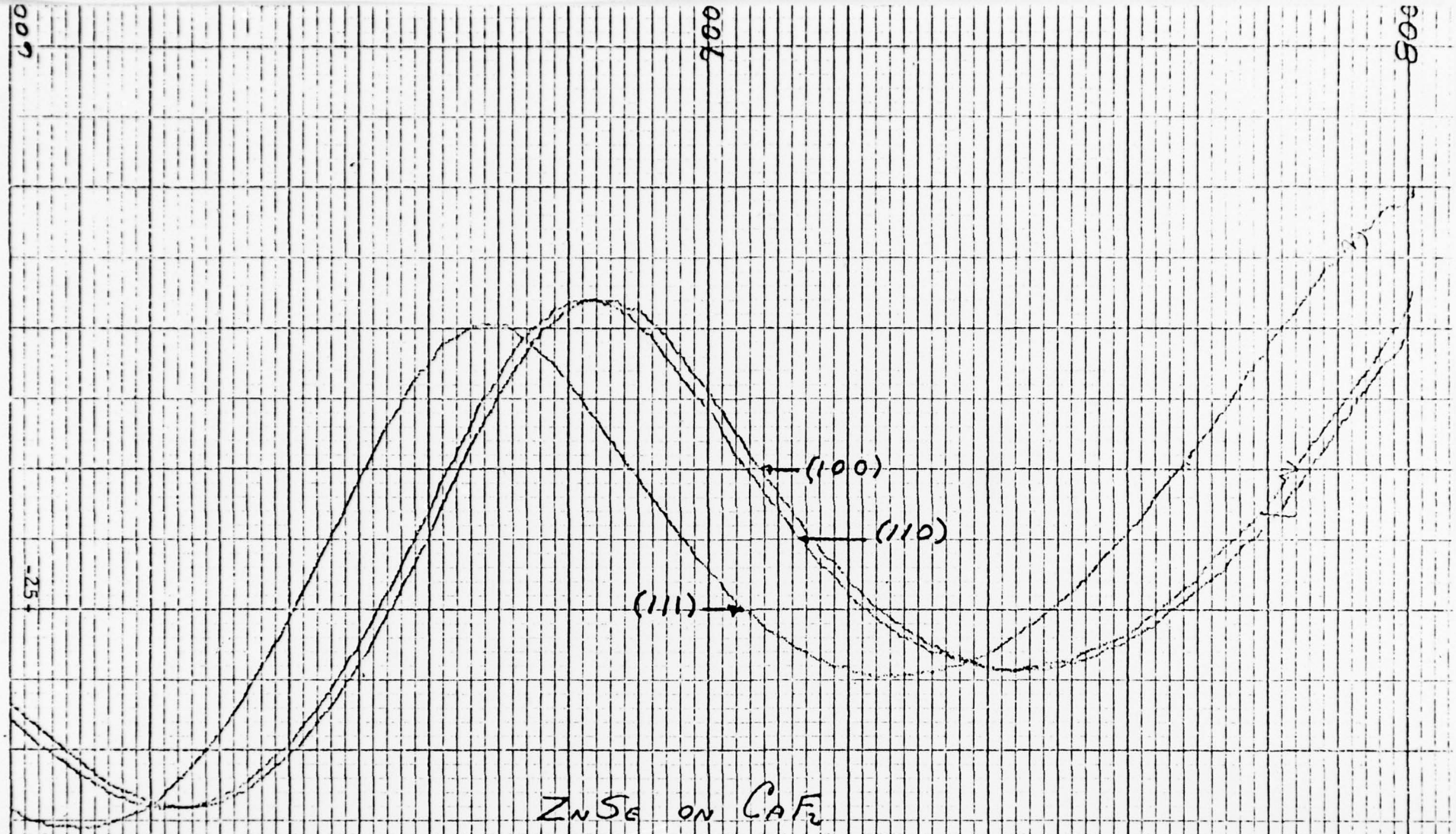

Figure 15. Spectrophotometer Scan of Zn Se on CaF_2 from 600 to 800 nm.

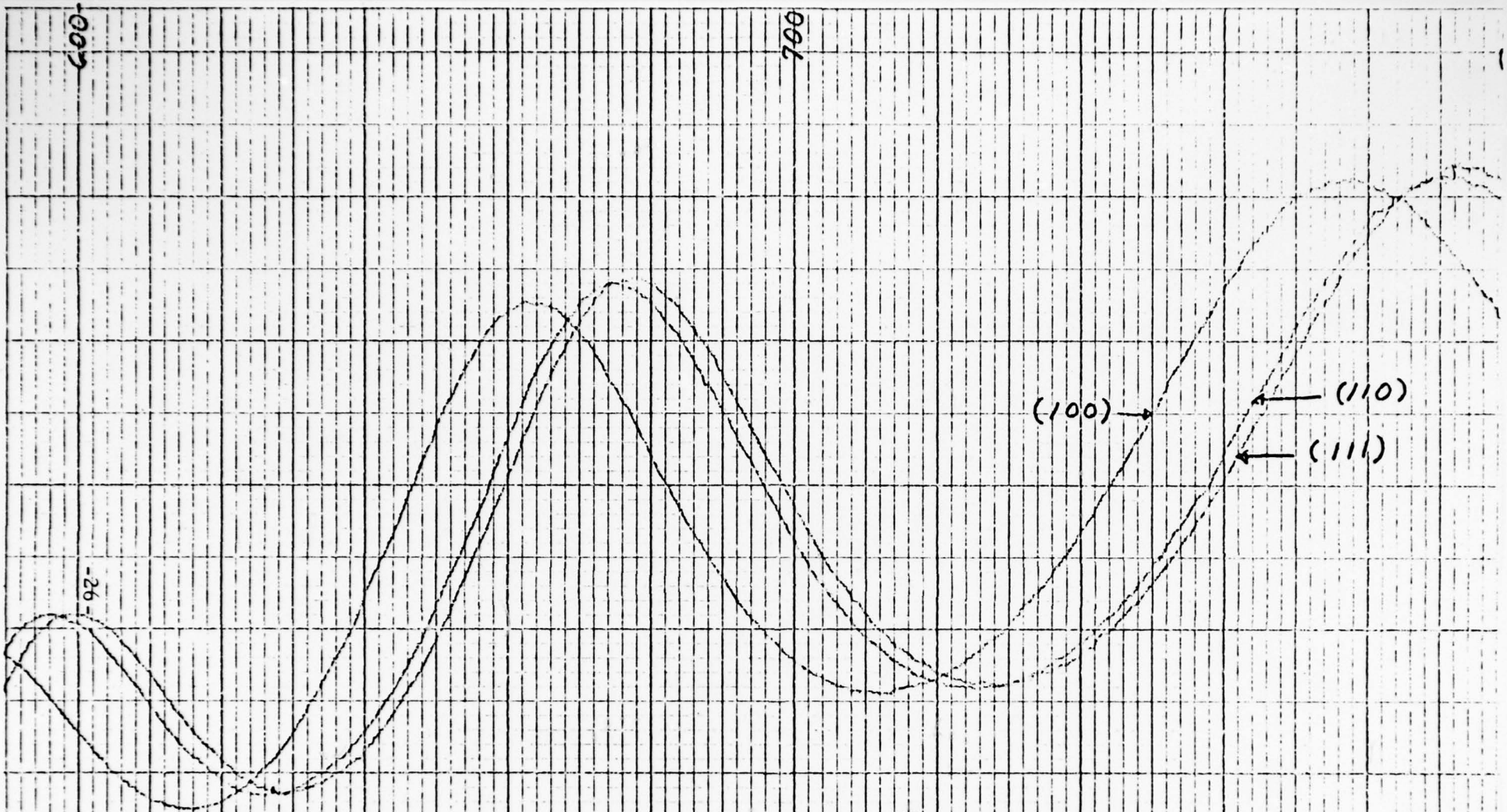

Figure 16. Spectropholometer Scan of Zn Se on SrF_2 from 600 to 800 nm.

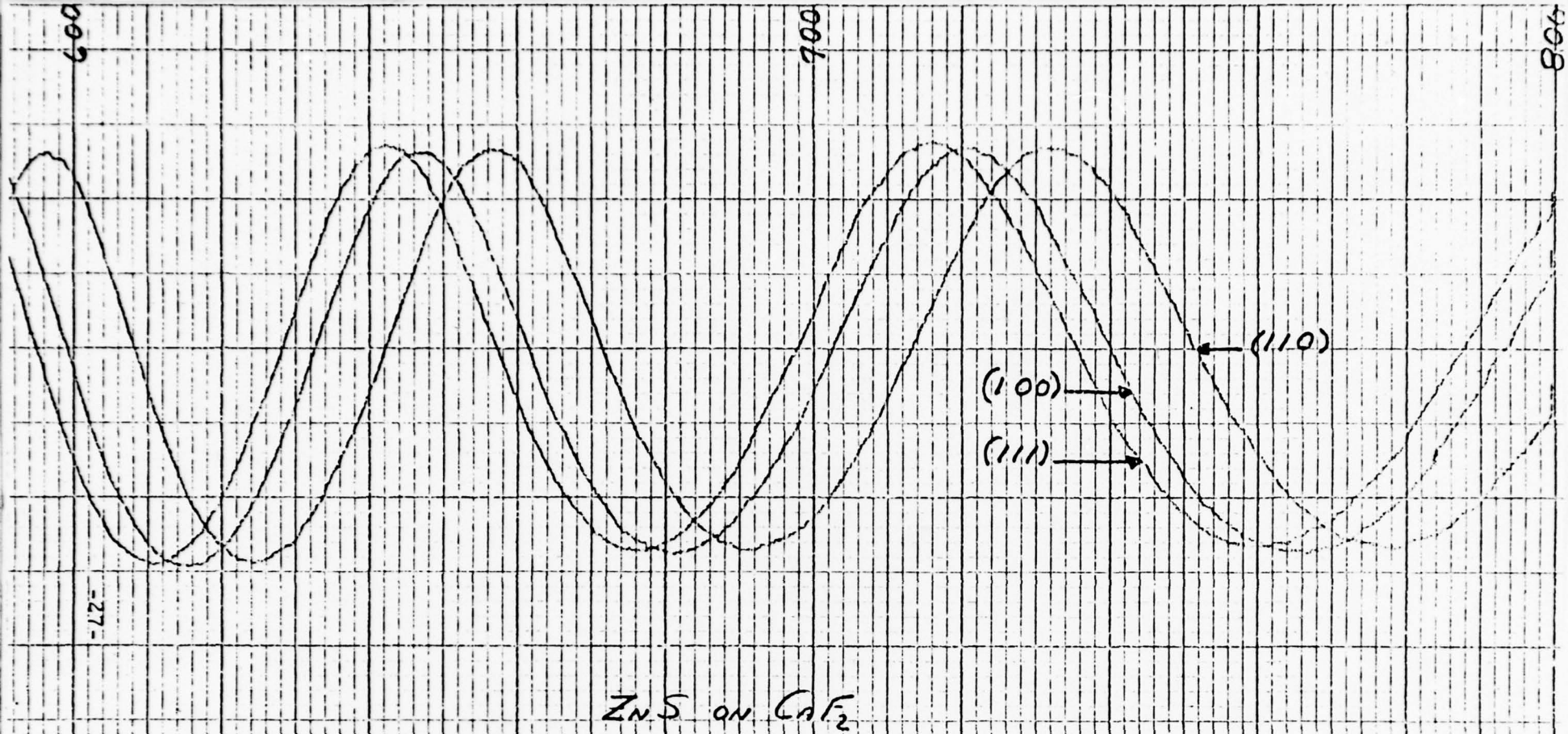

Figure 17. Spectrophotometer Scan of Zn S on Ca F_2 from 600 to 800 nm.

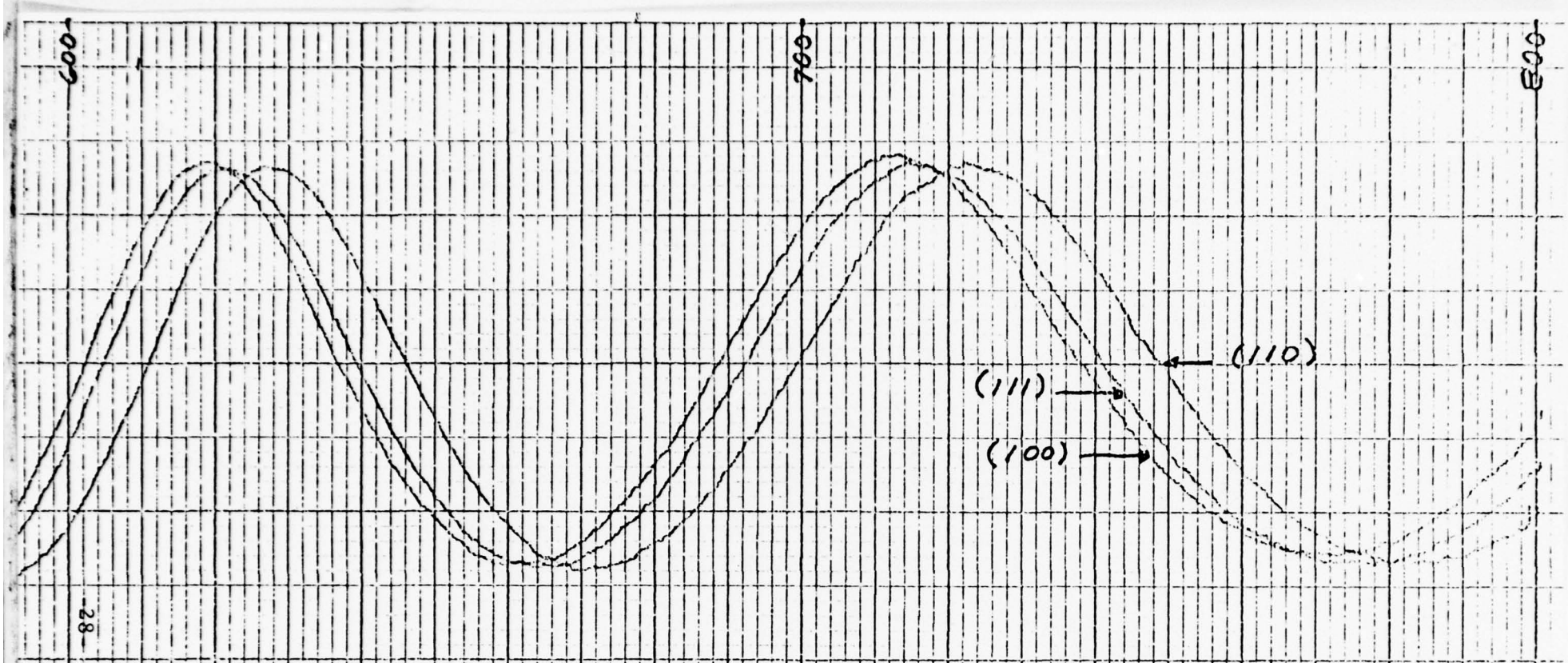

Figure 18. Spectrophotometer Scan of Zn S on $Sr F_2$ from 600 to 800 nm.

in optical thickness are proportional to differences in physical thickness and hence in growth rate of the coating material. Amplitudes of the maxima and minima in the transmission curves have no particular significance for this interpretation.

Considering individual materials, we see that growth rates for LaF_3, MgF_2, SrF_2, and ThF_4 on the three substrate orientations (figures 1-3 and 6-8) are indistinguishable by this method of measurement. For PbF_2 on CaF_2, (figure 4) the growth rate on the substrate oriented parallel to (110) is more rapid than on the substrate oriented parallel to (111), while growth of the PbF_2 film on the substrate oriented parallel to (100) is slowest of all. For brevity, we may symbolize this as (110) > (111) > (100). On SrF_2, the relative growth rates of PbF_2 are (110) > (100) > (110).

For Al_2O_3 on CaF_2 (fig. 9) the growth rate on (100) $\cong$ (110) > (111), while on SrF_2 (fig. 10) the growth rate on (110) > (100) $\cong$ (111). For MgO, (fig. 11 and 12) the growth rates on (110) and (111) are essentially equal on both CaF_2 and SrF_2 substrates. However, on CaF_2 the growth rate on (100) is more rapid than on the other two orientations while on SrF_2 the growth rate on (100) is slower than on (110) and (111). For SiO, the results were somewhat surprising in that no strong correlation of growth rate with substrate orientation was expected since the films are reputed to be amorphous. It is found that on CaF_2 (fig. 13), the growth rate on (100) > (111) > (110) while on SrF_2 (fig. 14), the growth rate on (110) $\cong$ (111) > (100). Results of x-ray diffraction studies of SiO on these substrates may indicate reasons for these differences.

ZnSe exhibits different growth rates on CaF_2 and SrF_2 (fig. 15 and 16). On CaF_2 the rates on (100) and (110) are essentially equal and more rapid than on (111), the slowest growth orientation. On SrF_2, the rates on (110) and (111) are approximately equal, while (100) is the slowest

growth orientation. For ZnS, (fig. 17 and 18) the growth rate on (110) is fastest on both CaF_2 and SrF_2. Growth rates of ZnS on (100) and (111) are nearly equal, with (100) being slightly faster on CaF_2 and (111) slightly faster on SrF_2. The significance of the growth rate results will become more apparent when correlated with absorption and structural data.

In order to obtain absorptance values (β and k) for halfwave thicknesses of coating materials, absorptances for the uncoated substrates must be known. The determination of the absorption coefficient of a coating material on a substrate which is transparent in the wavelength region of the irradiating laser is in principle quite straightforward. The total absorption due to a coating of specified thickness is obtained as a difference in total absorption between coated and uncoated substrates. Sequential measurements on the same substrate are utilized to obtain either a difference in absorption between coated areas or a difference in absorption in a single location before and after coating. The former method has the advantages of speed and ease of verification, but substrate inhomogeneity can cause difficulties. In the latter method, substrate inhomogeneith is eliminated, but verification of the absorption measurement on the uncoated substrate is problematic.

For an uncoated transparent substrate irradiated by a laser beam in a standard adiabatic calorimeter configuration, the total absorption A_o is given by[12]

$$A_o = \frac{2n_s}{1 + n_2^{\,2}} \quad P_A/P_T \qquad (1)$$

where n_s is refractive index of the sample, P_A is power absorbed by the sample, and P_T is the power transmitted through the sample. If the masses and heat capacities of the sample and calorimeter cone are

known and irradiation times are held constant for a given series of measurements, the absorption is proportional to the ratio of output voltages from the sample and power cone thermocouples.

The total absorptance calculated from (1) includes both surface and bulk contributions. The absorption coefficient for this substrate is

$$\beta = A_o / \ell \tag{2}$$

where ℓ is the sample thickness; again, both surface and bulk contributions are included. If a coating is subsequently deposited upon such a substrate and a new absorption measurement made, the total absorptance takes on a value

$$A_t = A_o + A_1 \tag{3}$$

where A_1 is the increase in total absorptance due to the coating alone. For the case of a coating of halfwave optical thickness, A_1 can be evaluated using (1) and (3) since the surface reflectivity of the coated sample is identical to that of the uncoated substrate and the parenthetical factor involving n_s in (1) remains unchanged.

To obtain an absorption coefficient for a coating of physical thickness t_1 from a measured value of A_1, we employ a formula of Loomis,[13] with minor rearrangement,

$$\beta_1 = \frac{A_1 n_1}{2 t_1 n_o} \quad \frac{(n_o + n_s)^2 \cos^2 \varphi_1 + [n_1 + (n_o n_s / n_1)]^2 \sin^2 \varphi_1}{n_1^2 + n_s^2}, \tag{4}$$

where

n_1 = film refractive index

n_s = substrate refractive index

n_o = incident medium refractive index

$\varphi_1 = 2\ n_1 t_1 /\ _o$

λ_o = laser wavelength (vacuum).

For a single coating of thickness $\lambda_o/2$, (4) reduces to

$$\beta_1 = \frac{A_1 n_1}{2 t_1 n_o} \quad \frac{(n_o + n_s)^2}{n_1^2 + n_s^2} \tag{5}$$

The absorption index of the thin film is then

$$k_1 = \frac{\lambda_o \beta_1}{4\pi} \tag{6}$$

Hence, in order to obtain the absorption coefficient and absorption index of a single layer coating on a transparent substrate, we require only the refractive index of film and substrate, the physical thickness of the film, and two absorption measurements. The method of measuring the absorption has been discussed in the literature.[14, 15]

The spectral composition of the irradiating laser has been shown to be a significant variable in absorptance measurements at CO laser wavelengths.[14, 16] In order to verify the spectral output of both the CO and DF lasers employed in the present measurements, spectra were analyzed using a Jarrell-Ash Model 78-466 scanning spectrometer with a 50 groove/mm grating blazed at 10.0 μm and a Ge:Au detector. Spectra for the CO laser have been reported previously,[14, 16]

with centroids varying from 5.25 μm to 5.45 μm, depending upon CO partial pressure. In the present study, with operating parameters typical of those employed in the calorimetric measurements (i.e. 6 mm intracavity iris, total output power ~2.8 W), the mean centroid of two spectra run with identical parameters was 5.29 ± .04 μm, with a bandwidth of 0.64 ± 0.1 μm.

The DF laser spectrum was analyzed in more detail since the actual output of the laser in use in the calorimetry laboratory had not been characterized previously. The same spectrometer, grating, and detector employed with the CO laser were used to analyze the DF. Typical operating parameters for calorimetric measurements were used. These include a helium partial pressure of ~4 Torr, with about 1.2 Torr each of SF_6 and D_2, and ~0.1 Torr of 0.2, for a total of 6-8 Torr. The discharge tube is operated at a voltage of ~13 kV and current of ~450 mA to produce 2-4W total power. Cavity temperature is ~65°C. Seven spectra were run over a three-day period and the results averaged to obtain a composite spectrum, presented in figure 19 and table 3.

In general, it appears that the overall spectrum is very stable with respect to centroid (~3.9 μm) and bandwidth (~0.3 μm), but individual lines are highly variable. Table 3 is an attempt at quantitative characterization of this aspect of the spectrum. In this table, the first column gives the wavelength of individual lines as measured with the spectrometer (in air). "Line Identification" (column 2) is obtained by comparison with published data.[17,18] Column 3 ($\bar{I}$) gives the mean relative intensity of each line. The tabulated number was obtained by first determining the intensity of the line in question in each of the seven spectra, relative to the strongest line in that spectrum taken as 1.0, and then averaging the results over all seven spectra. (If a line was absent

Fig. 19. DF LASER SPECTRUM COMPILED FROM 7 RUNS OVER A 3-DAY PERIOD, OUTPUT POWER: 2-4 WATTS.

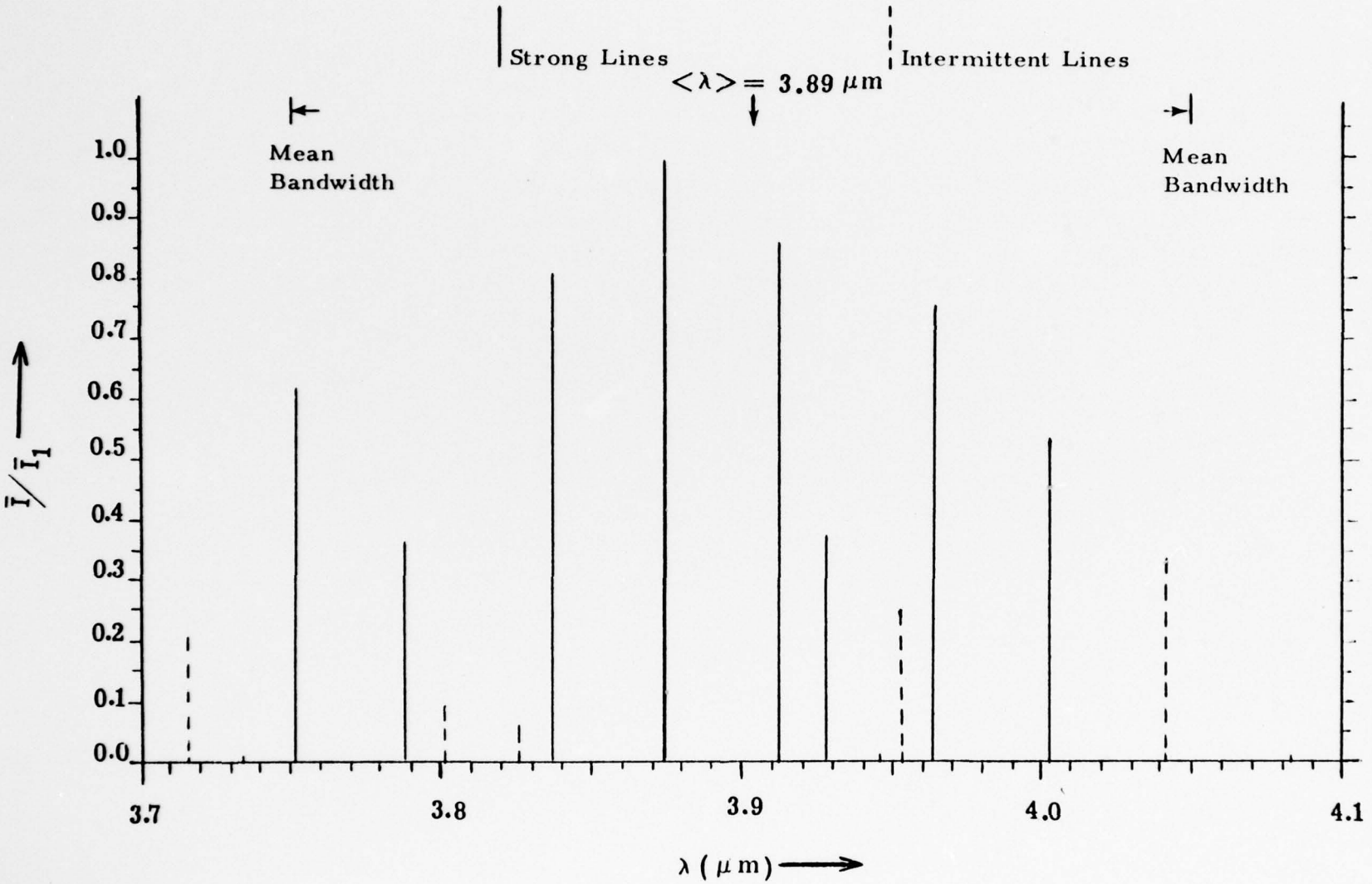

TABLE 3. DF Laser Spectrum Compiled from 7 Runs on 3 Days. Mean Centroid $\langle \lambda \rangle$ of All Spectra is 3.89 ± .025 μm. Mean Bandwidth of All Spectra is 0.297 μm ± 0.028 μm. For Individual Lines, Tabulated $\bar{\lambda}$ May Vary by ± 0.0007 μm From Run to Run.

$\bar{\lambda}$ (μm)	Line Ident.	$\bar{I}$	$\bar{I}/\Sigma\bar{I}$	$\lvert\Delta\bar{I}\rvert$	$\lvert\Delta\bar{I}\rvert/\Sigma\bar{I}$	$\bar{I}/\bar{I}_1$	No Runs Present
3.1760	1-0, P(9)	0.14	0.032	0.16	0.036	0.21	4
3.7514	1-0, P(10)	0.42	0.096	0.31	0.071	0.62	7
3.7880	1-0, P(11)	0.25	0.057	0.22	0.050	0.37	6
3.8262	1-0, P(12)	0.04	0.009	0.06	0.014	0.06	2
3.7337	2-1, P(6)	<0.01	<0.002	0.02	0.005	<0.01	1
3.8015	2-1, P(8)	0.07	0.016	0.12	0.027	0.10	2
3.8372	2-1, P(9)	0.55	0.125	0.42	0.096	0.81	7
3.8737	2-1, P(10)	0.68	0.155	0.27	0.062	1.00	7
3.9123	2-1, P(11)	0.59	0.134	0.38	0.087	0.86	7
3.9526	2-1, P(12)	0.18	0.041	0.19	0.043	0.26	4
3.9270	3-2, P(8)	0.26	0.059	0.25	0.057	0.38	5
3.9639	3-2, P(9)	0.52	0.118	0.33	0.075	0.76	7
4.0021	3-2, P(10)	0.36	0.082	0.28	0.064	0.53	6
4.0414	3-2, P(11)	0.30	0.068	0.40	0.091	0.44	4
4.0832	3-2, P(12)	<0.01	<0.002	0.02	0.005	<0.01	1
3.9457	4-3, P(5)	0.01	0.002	0.03	0.007	0.01	1

from a particular spectrum, its intensity was counted as 0.)

The mean relative intensities in column 3 of the table were divided by the sum of all of the mean intensities to obtain the fraction of the total laser energy in any given line, listed in the fourth column. The fifth column, headed "$\Delta\bar{I}$" gives the standard deviation of the mean relative intensities in column 3. This is divided by the sum of the intensities to determine the variability of a given line as a fraction of the total laser output and tabulated in the sixth column. In the seventh column, the mean relative intensity of each line is divided by that of the strongest line (2-1, P(10)), to obtain a relative intensity scale for plotting in figure 19. Note that this number is also the fraction of total laser energy appearing in an individual line, relative to the strongest line in the composite spectrum. Finally, the last column of the table designates the number of spectra, (out of a total of 7) in which an individual line had non-zero intensity.

Results of the coating absorptance measurements carried out to date under the contract are presented in tables 4-7, along with refractive indices determined from quarterwave films. The absorption coefficient, β, is tabulated rather than the absorption index, k, for convenience. The absorption index can of course be obtained from the β values using equation (6).

Some general features of the data are worth noting. It appears that the coating materials fall into three broad groups, based on absorption; (1) those having β values between ~ 0.5 and $\sim 5\ cm^{-1}$, (the low absorption group); (2) those having β values between ~ 7 and $\sim 11\ cm^{-1}$ (the intermediate group); and (3) those having β values of $13\ cm^{-1}$ or more, ranging up to $57\ cm^{-1}$ (high absorption group).

TABLE 4. ABSORPTION COEFFICIENTS OF FLUORIDE COATING MATERIALS MEASURED BY DF LASER CALORIMETRY ON COATINGS OF HALFWAVE OPTICAL THICKNESS AT A DESIGN WAVELENGTH OF 3.8 μm.

COATING MATERIAL	REFRACTIVE INDEX	COATING ABSORPTION COEFFICIENT, β (cm^{-1})					
		CaF_2 SUBSTRATE			SrF_2 SUBSTRATE		
		(100)	(110)	(111)	(100)	(110)	(111)
LaF_3	1.52	22.56	15.46	13.52	19.94	13.36	16.06
MgF_2	1.36	9.98	11.37	11.69	9.13	9.53	9.98
PbF_2*	1.73	2.41	1.73	4.08	1.51	3.08	2.84
SrF_2	1.34	20.75	23.13	15.13	--	--	--
ThF_4**	1.49	1.54	0.89	1.93	2.40	1.49	1.94

* ON CaF_2 THE GROWTH RATE OF PbF_2 ON (110) > (111) > (100), WHILE ON SrF_2, (110) ≥ (100) > (111).

** COATINGS ON ALL SUBSTRATES EMPLOYED CERAC RAW MATERIAL. GROWTH RATES OF ThF_4 ARE INDISTINGUISHABLE ON THE THREE ORIENTATIONS OF TWO SUBSTRATE MATERIALS.

TABLE 5. ABSORPTION COEFFICIENTS OF OXIDE, SULFIDE, AND SELENIDE COATING MATERIALS MEASURED BY DF LASER CALORIMETRY ON COATINGS OF HALF-WAVE OPTICAL THICKNESS AT A DESIGN WAVELENGTH OF 3.8 μm.

COATING MATERIAL	REFRACTIVE INDEX	COATING ABSORPTION COEFFICIENT, β (cm^{-1})					
		CaF_2 SUBSTRATE			SrF_2 SUBSTRATE		
		(100)	(110)	(111)	(100)	(110)	(111)
Al_2O_3	1.57	22.42	20.74	16.31	24.88	24.21	18.04
MgO	1.63	36.78	48.06	44.11	34.79	56.09	56.75
SiO	1.73	1.16	1.35	1.19	2.07	3.24	1.26
ZnSe	2.42	~0.99	~0.41	~0.80	0.72	2.48	3.11
ZnS	2.23	~3.61	~3.22	~2.88	10.70	8.64	12.54

Al_2O_3: ON BOTH SUBSTRATE MATERIALS THE GROWTH RATE ON (100) ≅ (110) > (111).

MgO: REFRACTIVE INDEX GIVEN FOR COATINGS ON CaF_2; ON SrF_2 n(100) = 1.62, n(110) = 1.66, n(111) = 1.65. ON CaF_2, THE GROWTH RATE ON (100) > (110) ≅ (111), WHILE ON SrF_2, (110) ≥ (111) > (100).

SiO: ON CaF_2, THE GROWTH RATE ON (100) > (111) > (110), WHILE ON SrF_2, (110) ≅ (111) > (100).

ZnSe: β VALUES ON CaF_2 ARE APPROXIMATE SINCE COATING THICKNESS = $\lambda/2$ AT 5.3 μm RATHER THAN 3.8 μm; ON CaF_2, THE GROWTH RATE ON (100) ≅ (111) > (111), WHILE ON SrF_2, (110) ≅ (111) > (100).

ZnS: β VALUES ON CaF_2 ARE APPROXIMATE SINCE COATING THICKNESS = $\lambda/2$ AT 5.3 μm RATHER THAN 3.8 μm; ON CaF_2, THE GROWTH RATE ON (110) > (100) > (111), WHILE ON SrF_2, (110) > (111) > (100).

TABLE 6. ABSORPTION COEFFICIENTS OF FLUORIDE COATING MATERIALS MEASURED BY CO LASER CALORIMETRY ON COATINGS OF HALFWAVE OPTICAL THICKNESS AT A DESIGN WAVELENGTH OF 5.3 μm.

COATING MATERIAL	REFRACTIVE INDEX	COATING ABSORPTION COEFFICIENT, β (cm^{-1})					
		CaF_2 SUBSTRATE			SrF_2 SUBSTRATE		
		(100)	(110)	(111)	(100)	(110)	(111)
PbF_2*	1.72	0.96	1.22	1.90	--	--	--
SrF_2	1.33	9.19	8.34	6.92	--	--	--
ThF_4**	1.48	1.74	1.13	1.61	0.76	0.42	0.42

* THE GROWTH RATE OF PbF_2 ON (110) > (111) > (110).

** COATINGS ON CaF_2 SUBSTRATES UTILIZED CERAC RAW MATERIAL; THOSE ON SrF_2 EMPLOYED BALZERS MATERIAL. GROWTH RATES ARE INDISTINGUISHABLE ON THE THREE ORIENTATIONS OF TWO SUBSTRATE MATERIALS.

TABLE 7. ABSORPTION COEFFICIENTS OF OXIDE, SELENIDE, AND SULFIDE COATING MATERIALS MEASURED BY CO LASER CALORIMETRY ON COATINGS OF HALFWAVE OPTICAL THICKNESS AT A DESIGN WAVELENGTH OF 5.3 μm.

COATING MATERIAL	REFRACTIVE INDEX	COATING ABSORPTION COEFFICIENT, β (cm^{-1}) CaF_2 SUBSTRATE (100)	(110)	(111)	SrF_2 SUBSTRATE (100)	(110)	(111)
SiO	1.78	36.95	39.42	37.50	--	--	--
ZnSe	2.41	2.61	0.63	1.11	1.16	1.38	1.35
ZnS	2.22	6.11	7.27	6.92	4.25	4.35	5.25

SiO: THE GROWTH RATE ON (100) > (110) ≅ (111).

ZnSe: ON CaF_2, THE GROWTH RATE ON (100) ≅ (110) > (111), WHILE ON SrF_2, (110) ≅ (111) > (100).

ZnS: ON CaF_2, THE GROWTH RATE ON (110) > (100) > (111), WHILE ON SrF_2, (110) > (111) > (100).

The sum of the standard deviation of the absorption measurements on the uncoated and coated substrate is a measure of the precision of the coating absorption determination. Since this determination involves the subtraction of two numbers with similar errors, the precision of the results will vary. The error in the coating absorption determination for the low absorption group is of the order of 10 to 15 %; that for the intermediate and high absorption groups is 3 to 5 %.

In general, differences among materials are greater than differences among substrate orientations for the same coating material. However differences among substrate orientations for the same coating may amount to factors of 2 to 4 (e.g. ZnSe on SrF_2 at 3.8 μm, Table 5, or on CaF_2 at 5.3 μm, Table 7). While it is tempting to correlate such differences in absorption coefficient with growth rate results, this correlation is of limited usefulness in the absence of structural data which are presently being gathered.

4. FUTURE PLANS

The coating structure and preferred orientation data presently being gathered will be completed and the deposition variables and environmental effects studies begun in the next quarter.

Five coating materials have tentatively been chosen for optimization of deposition conditions. These are PbF_2, ThF_4, ZnSe, and ZnS for use at both 5.3 μm and 3.8 μm, and SiO for 3.8 μm. In addition, the effect of glow discharge cleaning on surface absorption of SrF_2 substrates sill be investigated.

REFERENCES

1. J. T. Cox and G. Hass, "Antireflection Coatings for Germanium and Silicon in the Infrared", J. Opt. Soc. Amer., Vol. 48, p. 677 (1958).

2. G. Hass, and E. Ritter, "Optical Film Materials and Their Applications", J. Vac. Sci. and Tech., Vol. 4, p. 71 (1966).

3. Electron-Beam Technology, Airco-Temescal, Berkeley, California (1973).

4. M. G. Inghram, "Detection of Impurities", in Solid State Physics, L. Marton, Editor, Vol. 6, Chap. 2, Academic Press, N.Y., (1959).

5. L. Holland, Vacuum Deposition of Thin Films, Chap. 3, Chapman and Hall, London (1956).

6. J. F. Hall and W. F. C. Ferguson, "Optical Properties of Cadmium Sulfide and Zinc Sulfide from 0.6 microns to 14 Microns", JOSA, Vol. 45, p. 714 (1955).

7. R. J. Mattauch, "A Simple Vacuum Substrate Heater", Rev. Sci. Inst., Vol. 43, p. 148, (1972).

8. M. M. Hanson, P. E. Oberg, and C. H. Tolman, "Substrate-Temperature Measurement and Control", J. Vac. Sci. and Tech., Vol. 3, p. 277, (1966).

9. G. Hass and C. D. Salzberg, "Optical Properties of Silicon Monoxide in the Wavelength Region from 0.24 to 14.0 Microns", JOSA, Vol. 44, p. 181 (1954).

10. W. Steckelmacher, in Thin Film Microelectronics, L. Holland, Editor, p. 193, John Wiley & Sons, Inc., New York (1965).

11. K. H. Behrndt, in Physics of Thin Films, G. Hass and R. E. Thun, Editors, Vol. 3, p. 1, Academic Press, New York, (1966).

12. R. Weil, "Calculations of Small Absorption Coefficients From Calorimetric Experimental Data", Appl. Phys., Vol. 41, p. 3012, (1970).

13. J. S. Loomis, "Absorption in Coated Laser Windows", Appl. Opt. Vol. 12, p. 877, (1973).

REFERENCES

14. P. Kraatz, and P. J. Mendoza, "CO Laser Calorimetry for Surface and Coating Evaluation", Proc. Fourth Conf. on Infrared Laser Window Materials, p. 77, (1975).

15. T. F. Deutsch, "Research in Optical Materials and Structures for High Power Lasers", Final Technical Report, Raytheon Research Division, ARPA Order 1180 (1973).

16. Kraatz, P., Holmes, S. J., and Klugman, A., "Absorptance of Coated Alkaline Earth Fluoride Windows at CO Laser Wavelengths", Proc. Fifth Conf. on IR Laser Window Materials, DARPA, (1975).

17. Gross, R. W. F., and Bott, J. F., Eds. Handbook of Chemical Lasers, Wiley, N. Y., pp. 236-237 (1976).

18. Spencer, D. J., Beggs, J. A., and Mirels, H., "Small Scale CW HF (DF) Chemical Laser", J. Appl. Phys., Vol. 48, pp. 1206-1211, (1977).